IEICE TRANS. COMMUN., VOL.E91–B, NO.6 JUNE 2008

PAPER

A Method for Converting Amplitude Probability Distribution of Disturbance from One Measurement Frequency to Another

Yasushi MATSUMOTO[†a)], **Kaoru GOTOH**[†], *and* **Takashi SHINOZUKA**[††], *Members*

SUMMARY To estimate the impact of electromagnetic disturbances on multi-carrier wireless systems, a method for converting an amplitude probability distribution (APD) of disturbance measured at a frequency to be valid for another frequency is presented. The conversion uses two parameters, the receiver noise power of the APD measuring equipment and a scale factor that can be estimated from a measured disturbance spectrum. The method is based on the assumption that the difference in measurement frequency affects only the relative scale of the probability distribution of band-limited disturbance amplitude, and is applicable to disturbances of practically importance such as 1) continuous or pulse-modulated wideband Gaussian noise, 2) disturbance with a much narrower bandwidth than receiver bandwidth B, and 3) repetitive short pulses with similar waveforms with an interval much longer than $1/B$. The validity of the proposed method is examined by measurements of actual disturbances.

key words: *amplitude probability distribution, disturbance measurement, electromagnetic interference, emission limit*

1. Introduction

As various radio systems become more popular and the clock frequency of digital electronic appliances increases, it is becoming more important to establish appropriate limits for electromagnetic disturbance radiated from electronic equipment to protect radio services. Measuring the amplitude probability distribution (APD) of a disturbance has been shown to be a promising method of defining emission limits to protect digital wireless systems [1]–[5]. It has been demonstrated, theoretically and experimentally, that the APD of a disturbance correlates well with degradation in bit error rate (BER) caused by disturbance in various digital wireless systems [2]–[4].

To evaluate the degradation in BER in multi-carrier systems such as OFDM, BER must be evaluated in each sub-channel. The raw BER (at the input of an error correction decoder) of a multi-carrier system can be obtained simply by averaging the BER over the sub-channels. To do this, the disturbance APD must be obtained at all sub-carrier frequencies with a measuring receiver with a frequency selectivity that matches the sub-channel bandwidth. Unfortunately, there is currently no measuring equipment that can perform such an APD measurement. An alternative method is to measure APD channel-by-channel. However, a major drawback of this method is its very long measurement time, which we describe below. To obtain a reliable value for the APD down to a probability, $P_{\min}$, measurement time must be longer than the order of $(BP_{\min})^{-1}$ so that a sufficient number of independent samples can be measured. For example, with a bandwidth of 1 MHz and $P_{\min} = 10^{-6}$, measurement time should be longer than one second. If an OFDM signal has a total bandwidth of B_{OFDM} and is comprised of N subcarriers, subchannel bandwidth is B_{OFDM}/N. Hence, a measurement time of at least $N/(B_{\mathrm{OFDM}}P_{\min})$ is necessary for one subchannel, and $N^2/(B_{\mathrm{OFDM}}P_{\min})$ for measuring all subchannels. For evaluating an OFDM system with a large N, measurement time becomes too long. If disturbance properties vary with time, such a long measurement time may lead to inaccurate measurement results. It should also be noted that decreased measurement time causes increased $P_{\min}$, as mentioned above. This reduces the probability range of the APD.

In light of these facts, we developed a method of estimating the APD at a desired frequency from a measured APD at a certain frequency. It is impossible to conduct this conversion for general cases because measured APDs do not provide any information on the disturbance waveform or spectrum. In other words, limiting the type of disturbance makes it possible to develop a conversion algorithm. To obtain valid conversion results, it is necessary 1) to clarify necessary conditions of disturbance and 2) to judge if a disturbance fulfills the conditions. Moreover, 3) the parameters used for the conversion should be easily obtained by measurement. To make 2) and 3) possible, we assume that we can use a spectrum analyzer. This is a reasonable assumption because APD measuring equipment is usually used with a spectrum analyzer or installed in a spectrum analyzer as an add-on function [1]. It should be noted that this assumption is not equivalent to assuming a known waveform because a spectrum analyzer does not provide information about the phase spectrum and has a finite frequency resolution.

In the following section, Sect. 2, we present a method of converting an APD and a probability distribution function (PDF) of a disturbance at one frequency to those at another frequency. This method is based on an assumption that difference in the measurement frequency affects only the relative scale of the probability distribution of band-limited disturbance amplitude. In Sect. 3, we discuss the conditions of properties of disturbance necessary to obtain valid conversion results. In Sect. 4, experiments are conducted to examine the validity of the method.

Manuscript received March 29, 2007.
Manuscript revised September 18, 2007.

[†]The authors are with National Institute of Information and Communications Technology, Koganei-shi, 184-8795 Japan.
[††]The author is with Telecom Engineering Center, Matsudo-shi, 270-2222 Japan.
a) E-mail: ymatsumoto@nict.go.jp

DOI: 10.1093/ietcom/e91–b.6.2010

2. Conversion Method

2.1 APD Measured at Different Frequencies

A schematic diagram of an APD measuring receiver is shown in Fig. 1. The disturbance from equipment under test (EUT), $v(t)$, is input to a receiving band pass filter (BPF). We assume a tunable BPF at the RF stage of the receiver that has a center frequency f_c (= measurement frequency) and a bandwidth B (resolution bandwidth, $B \ll f_c$).

The band-limited disturbance $u(t, f_c)$ is given by a convolution integral of $v(t)$ with the impulse response of the BPF as:

$$\begin{aligned} \mathrm{Re}[u(t, f_c)] &= \mathrm{Re}[u(t)\exp(2\pi j f_c t)] \\ &= \mathrm{Re}\left[\int_{-\infty}^{\infty} h(\tau, f_c) v(t-\tau) d\tau\right], \\ h(t, f_c) &\equiv h_0(t)\exp(2\pi j f_c t). \end{aligned} \tag{1}$$

In Eq. (1), Re[*] denotes the real part of a complex number. $h(t, f_c)$ and $u(t, f_c)$ are the complex representations of the impulse response of the BPF and the band-limited disturbance, respectively. The envelope detector outputs the envelope amplitude, x, of the sum of the band-limited disturbance, u, and the receiver noise, n.

$$x(t, f_c) \equiv |u(t, f_c) + n(t, f_c)|\,. \tag{2}$$

where $n(t, f_c)$ represents a band-limited complex Gaussian noise whose real and imaginary parts are independent Gaussian random variables with zero mean and variance σ^2. We assume the receiver noise to be white, and hence σ^2 is independent of the measurement frequency, f_c.

The APD is defined by the part of time that the amplitude, x, exceeds a specified threshold level, y.

$$APD(y|f) \equiv prob(x > y) = \int_y^{\infty} P_x(x|f)dx. \tag{3}$$

Note that $P_x(x|f)$ denotes the PDF of x at a given measurement frequency of f. To analyze the dependence of $P_x(x|f)$ on f, we first consider the dependence of $P_u(u|f)$, which denotes the PDF of envelope amplitude $|u|$, on f in Sect. 2.1, then we develop a formula for conversion of P_x and APD in Sect. 2.2, taking the effect of receiver noise into account.

Let us suppose two APDs, $APD(y|f_0)$ and $APD(y|f_c)$, of a disturbance measured at different frequencies, f_0 and f_c, respectively. Note that receiver noise is ignored here, as mentioned above, so Eq. (2) reduces to $x = |u|$. Since the APD is a monotonically decreasing function of y, if the conversion of APD from f_0 to f_c is possible, it is generally conducted with the following form with a function g, which relates threshold y_0 to y_c, as shown in Fig. 2.

$$APD(y_c|f_c) = APD(y_0|f_0), \; y_c = g(y_0, f_c, f_0). \tag{4}$$

If we suppose the input disturbance is linearly amplified (or attenuated) from $v(t)$ to $av(t)$, the envelope amplitude of the band-limited disturbance, u, also changes at both measurement frequencies, from $|u(t, f_c)|$ to $a|u(t, f_c)|$, and $|u(t, f_0)|$ to $a|u(t, f_0)|$, respectively. Since the function g in Eq. (4) must be unchanged by this linear amplification of input disturbance, we have

$$APD(ay_c|f_c) = APD(ay_0|f_0), \; ay_c = g(ay_0, f_c, f_0). \tag{5}$$

Equation (5) shows that g is a linear function of the threshold value, y, and can be written as $g(y, f_c, f_0) = \gamma(f_c, f_0)y$ with a coefficient (or "scale factor") γ. Then Eq. (4) can be rewritten by

$$APD(\gamma y_0|f_c) = APD(y_0|f_0). \tag{6}$$

The scale factor, γ, is generally a function of the probability $APD(y_0|f_0)$. However, here, we make an assumption that γ is independent of the probability in order to develop a simple conversion method. This assumption means that difference in the measurement frequency affects only the relative scale of the probability distribution of band-limited disturbance amplitude, $|u|$. As shown in the next section, Sect. 3, this assumption is valid for several important types of disturbance. With this assumption, we can obtain a relationship of the PDF at two different frequencies by substituting the APD given by Eq. (6) into Eq. (3) and differentiating with respect to y_0.

$$P_u(u|f_c) = \frac{1}{\gamma} P_u\left(\frac{u}{\gamma}\middle| f_0\right). \tag{7}$$

Equation (7) means that the disturbance PDF is linearly

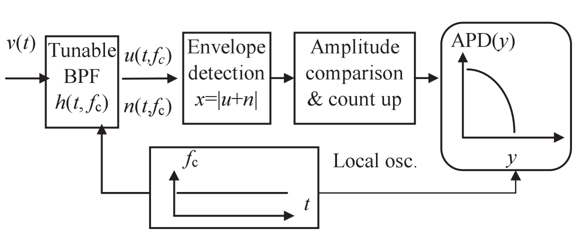

Fig. 1 Schematic diagrams of APD measuring receiver.

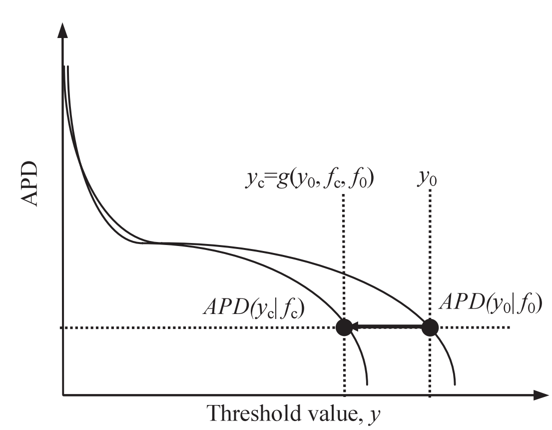

Fig. 2 Schematic illustration of conversion of a disturbance APD from a frequency $f = f_0$ to $f = f_c$.

converted from a measurement frequency f_0 to another frequency f_c with a scale factor γ. The following representation of the scale factor γ is obtained by taking the second moment of the amplitude of the band-limited disturbance $|u|$ using Eq. (7):

$$\gamma^2 = \sigma_d^2(f_c)/\sigma_d^2(f_0). \tag{8}$$

Note that $\sigma_d(f)$ is the variance of the band-limited disturbance $u(t, f)$ defined by Eq. (1). If the PSD, $P_0(f)$, of the disturbance $v(t)$ can be defined, the scale factor is also represented as

$$\gamma^2 = \frac{\sigma_d^2(f_c)}{\sigma_d^2(f_0)} = \frac{\int_0^\infty P_0(f)|H(f, f_c)|^2 df}{\int_0^\infty P_0(f)|H(f, f_0)|^2 df}, \tag{9}$$

where $H(f, f_c)$ denotes the transfer function of the BPF with a center frequency of f_c. It should be noted that $\sigma_d^2(f)$ represents the power of disturbance within the filter bandwidth of the measuring receiver, and hence we can estimate the scale factor, γ, by measuring the disturbance spectrum with a spectrum analyzer.

2.2 Conversion Formula

In the previous section, Sect. 2.1, we obtained Eq. (7), which relates the PDFs, between $f = f_0$ and f_c with a scale factor γ. Here, we should recall that the envelope amplitude, x, actually recorded as an APD, consists of disturbance u and receiver noise n, as given by Eq. (2), and that the PDF of receiver noise n cannot be converted with Eq. (7) because of the assumption of white Gaussian receiver noise.

Therefore, the next step is to represent the PDF, $P_x(x|f)$, with $P_u(u|f)$. Because of the assumption of white Gaussian receiver noise that is independent of received disturbance, the wanted PDF can be obtained by integrating the PDF of the Rice distribution with a weight of $P_u(u|f)$ [7], [8].

$$P_x(x|f) = \int_0^\infty P_u(u|f) P_{\text{Rice}}(x|u, \sigma^2) du, \tag{10}$$

$$P_{\text{Rice}}(x|u, \sigma^2) \equiv \frac{x}{\sigma^2} I_0\left(\frac{ux}{\sigma^2}\right) \exp\left(-\frac{x^2 + u^2}{2\sigma^2}\right).$$

In Eq. (10), $P_{rice}(x|u, \sigma^2)$ denotes the Rice PDF, which provides the conditional probability density of x for a given value of disturbance amplitude u. Note that σ^2 is the power of band-limited Gaussian receiver noise n. I_0 represents the zero order modified Bessel function of the first kind. Applying relationship (7) to Eq. (10) and changing integration variable u to $u' = u/\gamma$, we obtain the following:

$$P_x(x|f_c) = \int_0^\infty P_u(u|f_c) P_{\text{Rice}}(x|u, \sigma^2) du$$

$$= \int_0^\infty P_u(u'|f_0) P_{\text{Rice}}\left(x \mid \gamma u', \sigma^2\right) du.' \quad (u' \equiv u/\gamma) \tag{11}$$

To relate $P_x(x|f_c)$ to $P_x(x|f_0)$ in a simple closed form, we apply the Gaussian approximation of Rice distribution, which is valid if x is near to u and u is much larger than σ [11].

$$P_{\text{Rice}}(x|u, \sigma) \cong \frac{1}{\sqrt{2\pi\sigma^2}} \exp\left(\frac{-(x-u)^2}{2\sigma^2}\right) \equiv g(x-u|\sigma^2). \tag{12}$$

Note that $g(x - u|\sigma^2)$ represents a Gaussian PDF with mean u and variance σ^2. Using the approximation, the PDF, P_x, in Eq. (11) can be approximated by the following convolution.

$$P_x(x|f_c) \cong \int_{-\infty}^\infty P_u(u|f_0) g(x - \gamma u|\sigma^2) du. \tag{13}$$

As shown in Appendix A, we can obtain the formula for converting the PDF, from $P_x(x|f_0)$ to $P_x(x|f_c)$.

$$P_x(x|f_c) \cong \int_{-\infty}^\infty \frac{1}{\gamma} P_x\left(\frac{x-u}{\gamma} \,\middle|\, f_0\right) g(u|\sigma^2(1-\gamma^2)) du,$$

$$(x \gg \sigma,\ 1 > \gamma > 0)$$

$$g(x|\sigma^2(1-\gamma^2)) = \frac{1}{\sqrt{2\pi\sigma^2(1-\gamma^2)}} \exp\left(\frac{-x^2}{2\sigma^2(1-\gamma^2)}\right). \tag{14}$$

Equation (14) corresponds to processes of 1) linear compression of the amplitude scale of the PDF by factor γ, and 2) addition of Gaussian noise with a power of $(1 - \gamma^2)\sigma^2$, which compensates for the decrease in the receiver noise power from σ^2 to $\gamma^2\sigma^2$ caused by step 1).

By integrating Eq. (14) with respect to x from y to infinity, and then replacing the integration variable u to $u' = y - u$, we have the following formula for converting the APD:

$$APD(y|f_c) \cong \int_{-\infty}^\infty APD\left(\frac{u'}{\gamma} \,\middle|\, f_0\right) g(y - u'|\sigma^2(1-\gamma^2)) du'. \tag{15}$$

The scale factor γ in Eqs. (14) and (15) must be positive and less than unity, and hence the reference PDF should be measured at a frequency f_0 where the disturbance spectrum exhibits a maximum.

Since the above formula (15) is based on approximation (12), the accuracy of converted APD(y) becomes worse for smaller y. However, this does not significantly reduce the usefulness of the conversion formula (15), because of the following. To set the emission limit based on the estimation of BER, the disturbance amplitude at which the APD is on the same order as the required BER [3] is the most important. Required BER is generally much smaller than 1, e.g., 10^{-2} for voice communications, and 10^{-4} or less for data transmissions. This means that an $APD(y)$ for y close to the peak amplitude of the disturbance is important, but the loss of accuracy in $APD(y)$ for smaller y does not significantly affect the setting of emission limits, if the APD is measured with sufficient SNR. We did numerical calculations to find the SNR necessary for the approximation to be applied. Figure 3 compares APDs obtained by integrating the Rice PDF to those with the Gaussian approximation, for various signal powers. When the disturbance amplitude is 10 dB or more relative to the rms amplitude of the receiver noise, the difference between the exact and approximated APD is less than 0.1 dB at around the amplitude of the disturbance, which is sufficiently small for our purposes.

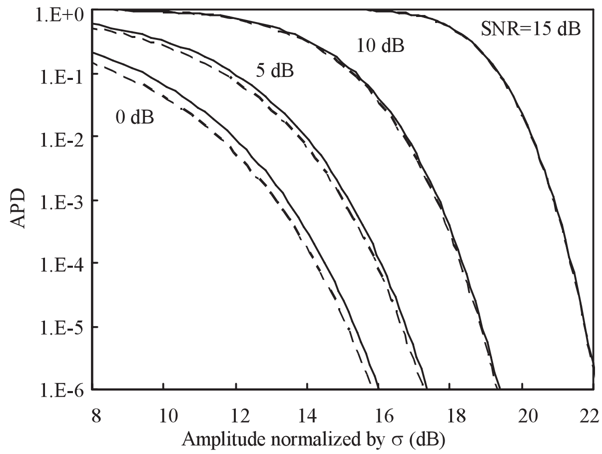

Fig. 3 Comparison of APDs of Rice distribution (solid lines) and approximation by Gauss distribution (broken lines) for various SNRs.

2.3 Conversion Procedure

(1) Measurement of receiver noise power

The receiver noise power, σ^2, is obtained by measuring the APD with a terminated RF input port of the receiver. Assuming the receiver noise to be Gaussian, the envelope amplitude has a Rayleigh PDF with $E(x^2) = 2\sigma^2$.

(2) Measurement of reference APD

Using a spectrum analyzer, disturbance spectrum is measured to find a reference frequency f_0, at which the spectrum shows the maximum. The reference APD is measured at f_0.

(3) Determination of scale factor

From the disturbance spectrum, the scale factor, γ, given by Eq. (9), is determined. For some types of disturbance, it becomes simpler, as shown in the following section, Sect. 3.

(4) Conversion of APD

Conversion is conducted with formula (15). Note that APD is usually measured as a function of quantized amplitude on a dB scale. Numerical integration of Eq. (15) should be conducted with care, as shown in Appendix B.

3. Conditions for Applying the Method

As mentioned in the previous section, to convert APD, we assumed Eq. (7). Hence, applicability of the proposed method and accuracy of conversion depends on 1) how exactly the disturbance of interest satisfies Eq. (7) and 2) how accurately the scale factor γ can be determined by measurement. In this section, we first discuss what types of disturbance satisfy condition (7), and then consider some other factors that may affect the applicability of the method.

3.1 Stationary Disturbance with a Stable Distribution

Here, we consider so-called stable distributions in probability theory. Assuming two independent random variables, v_1 and v_2, which have an identical PDF $P_v(v)$, if the PDF of a linear combination, $v = av_1 + bv_2$, (a and b are constant) can be represented with the original PDF, as $P_v(v/\gamma)/\gamma$, the distribution $P_v(v)$ is called strictly stable. Parameter γ is called the scale factor. For example, if two independent Gaussian random variables, v_1 and v_2, both of which have zero mean and variance of σ^2, a linear combination $v = av_1 + bv_2$ also has a Gaussian PDF with zero mean and variance of $\sigma^2(a^2 + b^2)$. In this example, the scale factor is $(a^2 + b^2)^{1/2}$.

Since the band-limitation with the BPF is a linear process, the above property can be applied to a disturbance with a stable distribution. If a disturbance $v(t)$ is stationary and has a strictly stable PDF, $P_v(v)$, the band-limited disturbance (the in-phase and quad-phase components of the complex envelope $u(t)$ in (1)) has a PDF that can be written in the form of $P_v(v/\gamma(f_c))/\gamma(f_c)$ for a tuned frequency, f_c. Accordingly, the PDFs of the envelope amplitude of the band-limited disturbance at different frequencies, $P_u(u|f_c)$ and $P_u(u|f_0)$, can be related as Eq. (7) with the scale factor $\gamma(f_c, f_0)$, which is given by $\gamma(f_c, f_0) = \gamma(f_c)/\gamma(f_0)$.

According to probability theory, there are infinite stable distributions. They generally have characteristic functions (CFs) that can be written in the form of $F(\xi) = \exp(-|c\xi|^\alpha)$ with constants c and α ($0 < \alpha \leq 2$) [6]. Gaussian distribution (in the case of $\alpha = 2$) is particularly important because it has a finite variance and hence scale factor is given by Eq. (9). If the input disturbance is stationary and Gaussian within the total bandwidth of interest, the envelope amplitude has a Rayleigh PDF that can be converted with the proposed method.

3.2 Narrowband Disturbances

If the disturbance has a center frequency f_0 and a bandwidth much narrower than the receiver bandwidth, B, the filtered disturbance can be approximated by the inputted disturbance weighted by the transfer function of the filter. Thus, the PDFs of the envelope amplitude of the band-limited disturbance at different frequencies can be related with Eq. (7), and the proposed method is applicable. Since the disturbance spectrum is much narrower than the resolution bandwidth, B, the scale factor given by Eq. (9) can be approximated by the frequency selectivity of the receiving filter, as $\gamma^2 = |H(f_0, f_c)/H(f_0, f_0)|^2$, and is independent of the waveform of the narrowband disturbance (shown in Fig. 4(a)).

3.3 Wideband Pulsed Disturbance

Since there are many disturbances that exhibit impulsive behaviors, we discuss the application of the proposed conversion method to pulse-modulated disturbance with duration Δ, much shorter than $1/B$. Such a disturbance is particularly important because it interferes with many subchannels of an OFDM signal simultaneously, which may cause significant degradation in BER [9].

Here, we define a wideband pulsed disturbance, $v(t)$,

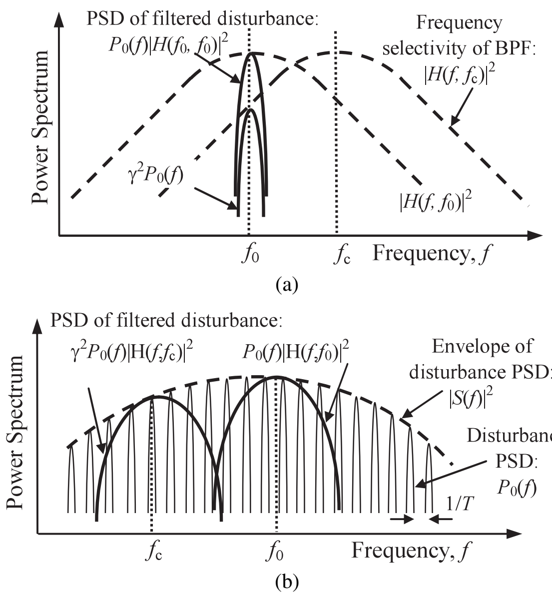

Fig. 4 Estimating scale factor γ. (a) Narrowband disturbance: $\gamma^2 = |H(f_0, f_c)/H(f_0, f_0)|^2$ (b) Wideband pulsed disturbance: $\gamma^2 = |S(f_c)/S(f_0)|^2$

as:

$$v(t) \equiv \sum_{n=-\infty}^{\infty} v_n(t - t_n), \quad t_n - t_{n-1} \equiv T_n \tag{16}$$

where $v_n(t)$ represents the pulse waveform that has nonzero values only at around $t = t_n$. Because of the above mentioned assumption that the pulse duration, Δ, is much shorter $1/B$, the complex envelope of the impulse response of the BPF, $h_0(t - t_n)$, can be approximated as constant within Δ. Furthermore, the amplitude of a disturbance pulse, $v_n(t-t_n)$, is assumed to be negligible for $|t-t_n| > \Delta/2$. Thus, the band-limited disturbance can be represented by:

$$\begin{aligned} u(t, f_c) &\cong \sum_{n=-\infty}^{\infty} \int_{tn-\Delta/2}^{tn+\Delta/2} h_0(t-\tau) \exp(2\pi j f_c(t-\tau)) v_n(\tau - t_n) d\tau \\ &\cong \sum_{n=-\infty}^{\infty} h_0(t-t_n) \exp(2\pi f_c(t-t_n)) \int_{tn-\Delta/2}^{tn+\Delta/2} v_n(\tau-t_n) \\ &\quad \cdot \exp(-2\pi j f_c(\tau-t_n)) d\tau \\ &\cong \sum_{n=-\infty}^{\infty} h(t - t_n, f_c) \int_{-\infty}^{\infty} v_n(\tau-t_n) \exp(-2\pi j f_c(\tau-t_n)) d\tau \\ &\cong \sum_{n=-\infty}^{\infty} h(t - t_n, f_c) S_n(f), \quad S_n(f) \equiv \mathcal{J}[v_n(t)]. \end{aligned} \tag{17}$$

Equation (17) indicates that the band-limited disturbance, $u(t, f_c)$, is represented by a train of impulse response pulses of the BPF, $h(t-t_n, f_c)$, weighted by the spectrum of disturbance pulse, $S_n(f)$.

We further assume that the repetition period of the disturbance pulses, T, is much longer than $1/B$, so that the band-limited disturbance becomes a train of non-overlapping pulses. This assumption is necessary for the disturbance to satisfy Eq. (7). Using a spectrum analyzer operated in the time sweep (zero span) mode, we can judge if the disturbance of interest satisfies this non-overlapping condition. The envelope amplitude, $|u(t, f_c)|$, under the condition is given by the sum of the amplitude of individual pulses.

$$\begin{aligned} |u(t, f)| &= \left| \sum_{n=-\infty}^{\infty} h(t - t_n, f) S_n(f) \right| \\ &= \sum_{n=-\infty}^{\infty} |h_0(t - t_n)| \, |S_n(f)|. \end{aligned} \tag{18}$$

It should be noted that the amplitude spectrum, $|S_n(f)|$ is a random variable if $v_n(t)$ is a sample waveform of a random process, so we define a PDF, $w_n(S|f)$, which represents the probability density of $|S_n(f)|$ at a frequency f. We also define the PDF of the envelope amplitude of the filter's impulse response, $|h_0(t - t_n)|$, in the period of $[(t_n - t_{n-1})/2, (t_{n+1} - t_n)/2]$, as $P_h(u)$. Then, the PDF of the envelope amplitude $|u(t, f)|$ within the above-mentioned period, P_n, is obtained by integrating $P_h(u)$ with a weight of w_n as,

$$\begin{aligned} P_n(u|f) &= \int_0^{\infty} \frac{1}{S} P_h\left(\frac{u}{S}\right) w_n(S|f) dS. \\ &\quad ((t_n - t_{n-1})/2 \le t < (t_{n+1} - t_n)/2) \end{aligned} \tag{19}$$

In Eq. (19), $P_h(u/S)/S$ corresponds to the conditional probability density of the envelope amplitude of the filter's impulse response pulse weighted by a given value of the amplitude spectrum S. Because of the above-mentioned non-overlapping assumption, the PDF of disturbance amplitude $|u|$ can be obtained by averaging P_n, over n.

$$\begin{aligned} P_u(u|f) &= \int_0^{\infty} \frac{1}{S} P_h\left(\frac{u}{S}\right) w(S|f) dS, \\ w(S|f) &\equiv \lim_{N\to\infty} \frac{1}{2N+1} \sum_{n=-N}^{N} w_n(S|f). \end{aligned} \tag{20}$$

By applying the relationship (20) to Eq. (7) and replacing the variable $S\gamma$ by S', we find the following condition is necessary,

$$w(S|f_c) = \frac{1}{\gamma} w\left(\frac{S}{\gamma}\middle| f_0\right). \tag{21}$$

In the following, we first take a simple example with a deterministic disturbance waveform, and then extend the discussion to disturbances with random waveforms.

(1) Repetition of similar pulse waveforms weighted by random amplitude coefficient

It is assumed that disturbance $v(t)$ is a train of an identical waveform $v_0(t)$ weighted by a random coefficient a_n. From Eq. (18), the envelope amplitude of the band-limited disturbance, $|u|$, is given by,

$$|u(t, f)| = |S_0(f)| \sum_{n=-\infty}^{\infty} a_n |h_0(t-t_n)|, \;\; S_0(f) \equiv \mathcal{J}[v_0(t)]. \tag{22}$$

It can easily be seen from Eq. (22) that the band-limited waveforms $|u(t, f_c)|$ and $|u(t, f_0)|$ are in a similarity relationship (i.e. $|u(t, f_c)| = \gamma|u(t, f_0)|$), and their PDFs satisfy Eq. (7). Thus, we can apply the conversion method to this type of pulsed disturbance. In this case, γ^2, given by Eq. (9), is approximately given by the normalized power spectrum of the single disturbance pulse, $|S_0(f_c)|^2/|S_0(f_0)|^2$, which represents the spectral envelope of the PSD, $P_0(f)$, because of our assumptions of $1/T \ll B \ll 1/\Delta$, as illustrated by Fig. 4(b). We also note that the above results are valid even when the disturbance pulse has a random time jitter, δ ($\ll T_n/2$), or a random phase because the jitter does not affect amplitude spectrum $|S_0(f)|$.

(2) Pulse modulated random waveform

We consider a disturbance generated by pulse modulating a wideband stationary noise with a bandwidth B_v. Note that the modulating pulse has a deterministic waveform and that the pulse duration, Δ, satisfies the following condition.

$$B_v \gg 1/\Delta \gg B. \tag{23}$$

Condition $B_v \gg 1/\Delta$ means that a sufficient number of independent samples are included in one pulse $v_n(t)$. Since the Fourier transform is a linear process, we can apply the property of stable distribution discussed in Sect. 3.1. Actually, it is known that PDF of the amplitude spectrum of a Gaussian noise modulated with a rectangular pulse can be asymptotically approximated by the following Rayleigh distribution if $B_v \gg 1/\Delta$ [7].

$$w(S|f_c) \cong \frac{S}{\Delta P_0(f_c)} \exp\left(-\frac{S^2}{2\Delta P_0(f_c)}\right), \tag{24}$$

where $P_0(f)$ is the PSD of the Gaussian noise before pulse modulation. Since the PDF of the spectrum given by (24) fulfills condition (21), the proposed conversion method is applicable to the pulsed Gaussian noise. In this case, the square of scale factor γ^2 can be approximated by the ratio of the PSD before pulse modulation, $P_0(f_c)/P_0(f_0)$ because of our assumption of $B_v \gg B$.

A Gaussian receiver noise mixed with such a pulse-modulated wideband Gaussian noise is known as the ε-mixture noise model, which is commonly used to analyze interference problems in wireless systems [10].

3.4 Other Factors Affecting the Applicability of the Method

In addition to the properties of disturbance mentioned in the previous sections, we should consider some factors that may affect the applicability of the proposed method from a more practical viewpoint.

(1) Interference with adjacent disturbance spectrum

Assume that there is a disturbance spectrum that is adjacent to or partially overlaps with the disturbance of interest. Even though each of two band-limited disturbances satisfies Eq. (7), their sum generally does not. Hence, converting APD into the border frequency of the two disturbance spectra may return an inaccurate result. It should be noted in such cases that the frequency selectivity of the BPF that determines the resolution bandwidth (shown as "tunable BPF" in Fig. 1) also affects the accuracy of conversion.

(2) Determination error of the scale factor

Equation (9) shows that the scale factor can, in principle, be determined using the PSD of the disturbance. However, in practice, the disturbance spectrum must be measured in a finite time, which means that the measured spectrum is not exactly equal to the spectrum defined by the Fourier transform. For example, if a disturbance consists of short pulses with a long pulse interval, it takes a long time to measure a disturbance spectrum that can be used to determine the scale factor accurately. As mentioned in Sect. 1, even though a short measurement time is preferable, a measurement time that is too short increases the error in the scale factor, degrading the accuracy of conversion.

It should also be noted that $P_0(f)$ in Eq. (9) is the PSD of the received disturbance $v(t)$ (not including the receiver noise), while the actually measured spectrum always includes receiver noise. In the frequency range where the disturbance PSD, $P_0(f)$, is not sufficiently higher than that of the receiver noise, (i.e. insufficient SNR) determination of the scale factor is not as accurate. As the disturbance PSD decreases, the APD of the sum of the received disturbance pulse and the receiver noise asymptotically approaches a known distribution, i.e. the Rayleigh APD of the receiver noise. Therefore, we can use the APD of the receiver noise as an approximation of the converted APD when the scale factor is very small. It is also important to note that disturbance APD at such a frequency with a low value of the disturbance PSD makes a relatively small contribution to the degradation in the total BER of an OFDM system.

Considering above-mentioned (1) and (2), conversion accuracy can be improved by dividing the frequency band of interest into multiple sub-bands (with a bandwidth wider than the subcarrier spacing of the OFDM), and then by applying the proposed method within each sub-band. This is a trade off, i.e., the finer the frequency band is divided, the better the conversion accuracy, but the longer measurement time required to obtain the reference APD for all sub-bands.

4. Experiments

We conducted experiments to compare converted APDs with measured ones. Figure 5 shows the frequency selectivity of the APD measuring receiver.

The resolution bandwidth was 1 MHz in terms of impulse bandwidth, which corresponded to a −3 dB-bandwidth of 0.66 MHz [5].

A narrowband disturbance was generated by band-limiting repetitive tone bursts with a Gaussian BPF. The APDs measured at various frequencies (indicated in Fig. 5) are plotted in Fig. 6 (thin lines), with the converted APDs (thick lines) from the reference APD measured at f_0. The

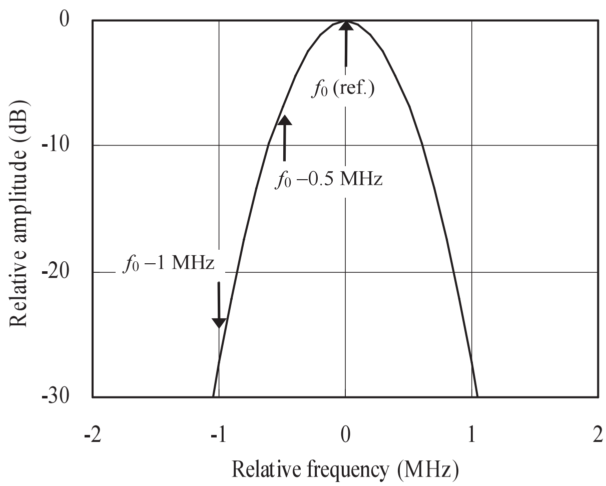

Fig. 5 Frequency selectivity of APD measuring receiver. Impulse bandwidth = 1 MHz, Gaussian filter.

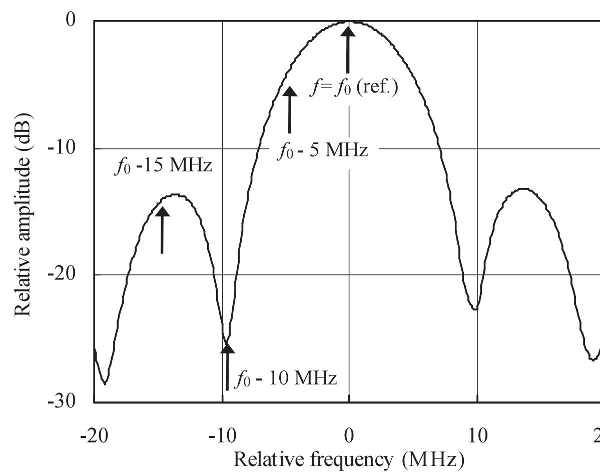

Fig. 7 Measured spectrum of a train of repetitive wideband pulses. Disturbance pulse duration: 0.1 μs, repetition frequency: 100 kHz. Resolution bandwidth: 1 MHz.

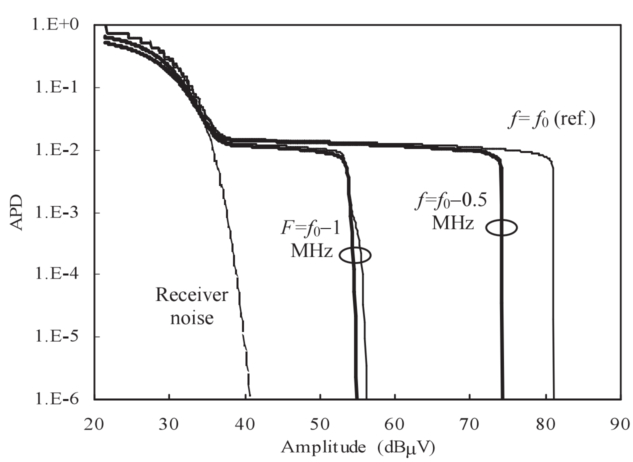

Fig. 6 Measured (thin lines) and converted (thick lines) APDs of repetitive narrowband pulses. Measured APD at $f = f_0$ was used as reference. Pulse duration: 10 μs, filtered by Gaussian BPF (B = 0.3 MHz), repetition frequency: 1 kHz. Resolution bandwidth: 1 MHz.

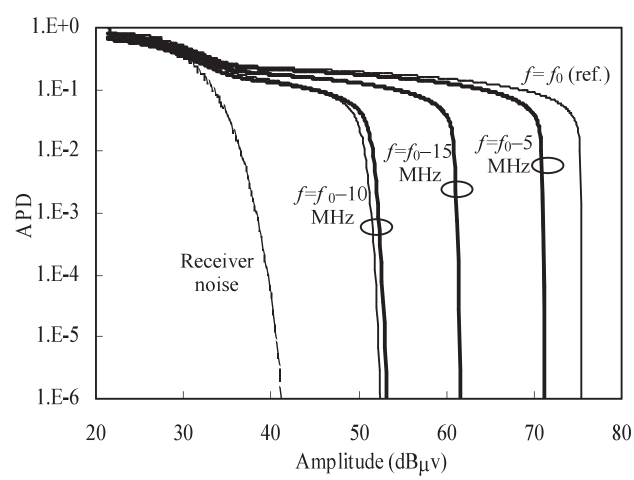

Fig. 8 Measured (thin lines) and converted (thick lines) APDs of repetitive wideband pulses. Measured APD at $f = f_0$ was used as reference. Pulse duration: 0.1 μs, repetition frequency: 100 kHz, and resolution bandwidth: 1 MHz.

converted APDs agree very well with the measured ones. A train of repetitive tone bursts without band-limitation was then applied as a wideband disturbance. Figure 7 illustrates the spectrum measured with a spectrum analyzer with a bandwidth of 1 MHz operated in peak detection mode. The converted APDs are found to be in good agreement with the measured ones, as shown in Fig. 8.

As the next step, we measured an actual disturbance from two types of personal computers, PC#1 and PC#2. APD measurement of the real disturbances was made channel by channel, assuming the properties of the disturbances did not vary with time.

Figure 9 illustrates the spectrum of a clock harmonic of PC#1, as an example of narrowband disturbance. The spectrum shows nearly the same bandwidth as the resolution bandwidth (1 MHz) since this PC#1 did not use a frequency-modulated (FM) clock signal. The periodic spikes found in the figure were not line spectral components but were caused by a periodic modulation in amplitude of the disturbance. Since the disturbance is narrowband, we can determine the scale factor, γ, with the frequency selectivity of the filter shown in Fig. 5. Measured and converted APDs are compared in Fig. 10 and found to be within a difference of 1 dB in the probability range from 10^{-2} down to 10^{-6}.

As an example of wideband disturbance, a clock harmonic from PC#2 was measured. The disturbance spectrum, measured in the peak detection mode, is shown in Fig. 11. Since PC#2 uses a frequency-modulated clock signal, its harmonic has a rapid frequency variation. As a result, the band-limited disturbance becomes repetitive impulse response pulses of the filter [12]. Hence, we can regard the FM harmonic as equivalent to a wideband pulsed disturbance. The scale factor for converting the APD was determined by the averaged disturbance spectrum shown in the thick curve in Fig. 11.

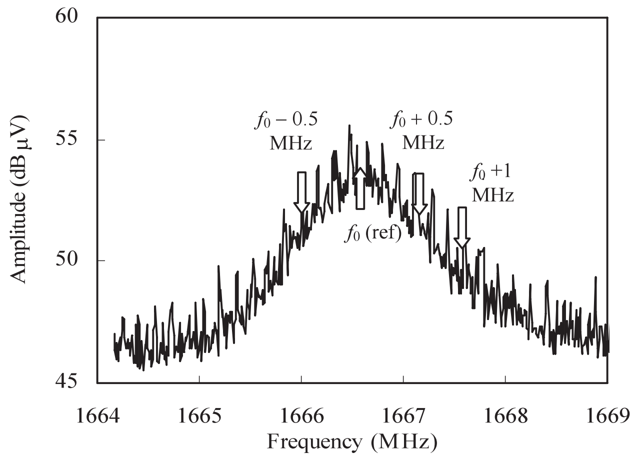

Fig. 9 Measured spectrum of a narrowband disturbance from PC#1 (clock harmonic without FM). Resolution bandwidth: 1 MHz, peak detection mode.

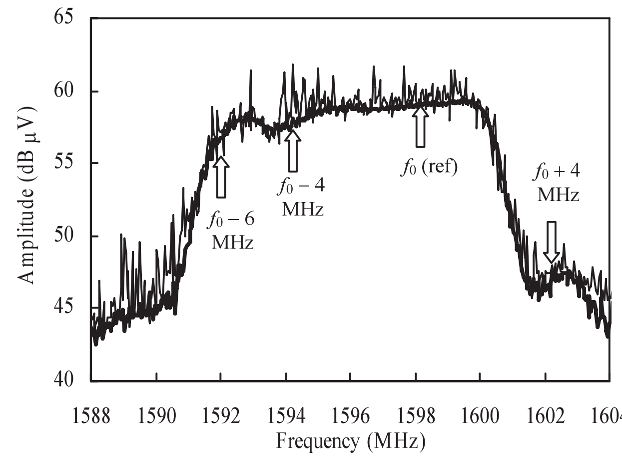

Fig. 11 Measured spectrum of a wideband disturbance from PC#2 (a harmonic of bus clock with FM). Resolution bandwidth: 1 MHz, peak detection mode. Thick curve indicates averaged spectrum.

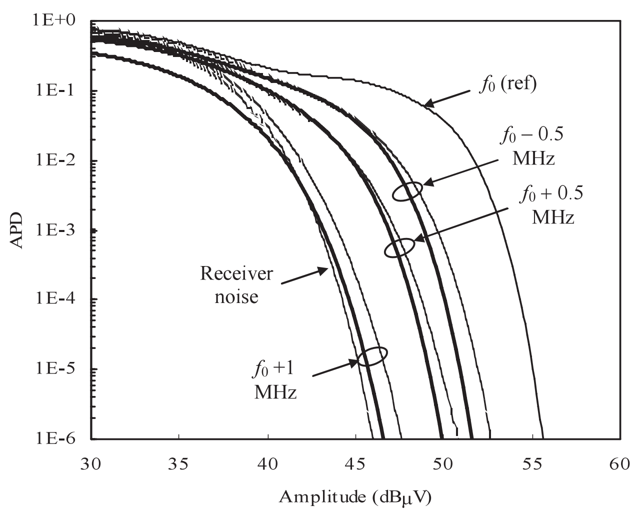

Fig. 10 Measured (thin lines) and converted (thick lines) APDs of narrowband disturbance from PC#1 (spectrum is shown by Fig. 9). Measured APD at $f = f_0$ was used as reference. Resolution bandwidth: 1 MHz.

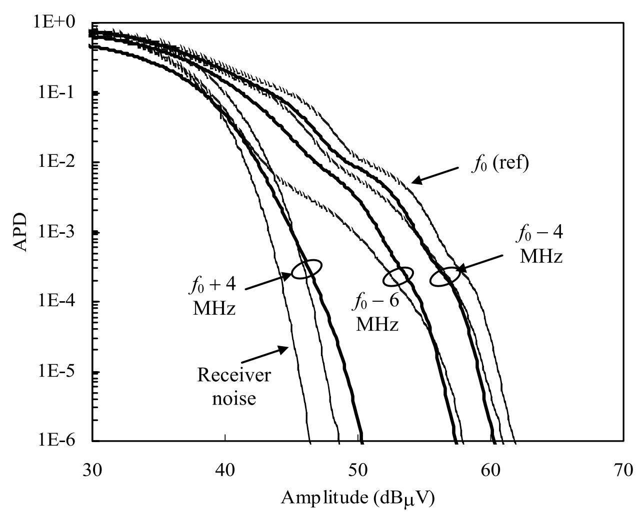

Fig. 12 Measured (thin lines) and converted (thick lines) APDs of wideband disturbance from PC#2 (the spectrum is shown by Fig. 11). Measured APD at $f = f_0$ was used as reference. Resolution bandwidth: 1 MHz.

As shown in Fig. 12, it was found that the converted APD at $f_0 - 6$ MHz is considerably larger than the measured one in the range from 10^{-1} to 10^{-3}. This is because the disturbance pulses at the output of the BPF do not satisfy the non-overlapping condition when the measurement frequency is at the edge of the harmonic spectrum, i.e. at around the maximum frequency deviation of the FM harmonic as shown in [12]. The overlapping between adjacent pulses actually decreases the duty ratio of the pulse train, while the overlapping is not assumed in the conversion algorithm, as mentioned in the previous section.

Hence, the converted APD shows larger probability than measured one (i.e. the worst-case estimation). Except for the above case of $f_0 - 6$ MHz, estimated APDs are found to be good approximations of the measured ones within a difference of 1.5 dB. One possible cause of the difference between the converted and measured APDs for actual disturbance is estimation error of the scale factor used for the conversion. Another possibility is the variation in the power and spectrum of the disturbances during the measurement. Since some background processes in the PC are initiated or terminated automatically, they can affect radiating power and spectrum of the clock harmonic.

These experimental results demonstrate that the proposed method is applicable to disturbances that satisfy the conditions shown in the previous section.

There are too many factors involved to draw a general conclusion about the accuracy of conversion necessary to evaluate the BER of an OFDM system. These include the tolerable error in the estimated BER, the total number of subchannels, minimum received power of the OFDM signal, etc. Considering that the amplitude accuracy of the APD measuring receiver is specified by CISPR as ±2.7 dB, including the RF section [5], this value can be regarded as a reference for discussing the accuracy of conversion.

5. Conclusion

A simple method for converting a disturbance APD from a measured frequency to another frequency was proposed, and the validity of the method was demonstrated by experiments. The conversion uses two parameters, the receiver noise power of the APD measuring equipment and a scale factor estimated by a measured disturbance spectrum. The method is based on the assumption that the difference in measurement frequency affects only the relative scale (scale factor) of the amplitude probability distribution of band-limited disturbance. It was shown that the method was applicable to such disturbances as 1) continuous or pulse-modulated Gaussian noise, 2) disturbance with a much narrower bandwidth than resolution bandwidth B, and 3) repetitive short pulses with similar waveforms with an interval much longer than $1/B$. However, it cannot be said that the application of the method is limited only to the above disturbance types. For example, it is considered that the method is applicable to a disturbance with a general case of stable distribution, as mentioned in 3.1, if the scale factor can be determined by measuring some statistical parameters of disturbance [13]. Investigation to the application of the proposed method to such disturbance types is a future work.

References

[1] M. Uchino, O. Taguchi, and T. Shinozuka, "Real-time measurement of noise statistics," IEEE Trans. Electromagn. Compat., vol.43, no.4, pp.629–636, Nov. 2001.
[2] Y. Yamanaka and T. Shinozuka, "Measurement and estimation of BER degradation of PHS due to electromagnetic disturbance from microwave ovens," IEICE Trans. Commun. (Japanese Edition), vol.J79-B-II, no.11, pp.827–834, Nov. 1996.
[3] K. Wiklundh, "Relation between the amplitude probability distribution of an interfering signal and its impact on digital radio services," IEEE Trans. Electromagn. Compat., vol.48, no.3, pp.537–544, Aug. 2006.
[4] K. Gotoh, S. Ishigami, Y. Matsumoto, T. Shinozuka, and Y. Yamanaka, "Electromagnetic disturbance measurement by using amplitude probability distribution for protecting digital wireless communication systems," J. National Institute of Information and Communications Technology, vol.53, no.1, pp.81–90, March 2006.
[5] CISPR 16-1-1 am. 1, 2005, Specification for radio disturbance and immunity measuring apparatus and methods, Part 1-1: Radio disturbance and immunity measuring apparatus and methods.
[6] M. Shao and C.L. Nikias, "Signal processing with fractal lower order moments: Stable processes and their applications," Proc. IEEE, vol.81, no.7, pp.986–1010, July 1993.
[7] D. Middleton, An introduction to statistical communication theory, Chap. 9, McGraw Hill, New York, 1960 (reprint ed., Wiley-IEEE Press, 1996).
[8] C. Loo, "A statistical model for a land mobile satellite link," IEEE Trans. Veh. Technol., vol.34, no.3, pp.122–127, Aug. 1985.
[9] Y. Matsumoto, T. Shimizu, T. Murakami, K. Fujii, and A. Sugiura, "Impact of frequency modulated harmonic noises on OFDM-based WLAN systems," EMC Europe 2006, pp.817–822, Barcelona, Sept. 2006.
[10] K. Vastola, "Threshold detection in narrow-band non-Gaussian Noise," IEEE Trans. Commun., vol.32, no.2, pp.134–139, Feb. 1984.
[11] S. Stein and J.J. Jones, Modern Communication Principles—With Application to Digital Signaling, Chap. 4, McGraw Hill, New York, 1968.
[12] Y. Matsumoto, K. Fujii, and A. Sugiura, "Estimating the amplitude reduction of harmonic spectra due to c lock frequency modulation," IEEE Trans. Electromagn. Compat., vol.48, no.4, pp.734–741, Nov. 2006.
[13] M. Shao and C.L. Nikias, "Signal processing with fractional lower order moments: Stable processes and their applications," Proc. IEEE, vol.81, no.7, pp.986–1010, July 1993.

Appendix A

The characteristic function (CF) of a Gaussian PDF is given by

$$\mathcal{J}\left[g(x-u|\sigma^2)\right] = \exp\left(\frac{-\xi^2\sigma^2}{2}\right)\exp(-j\xi u). \qquad \text{(A· 1)}$$

Using Eq. (A· 1), the CF, $F(\xi|f_c)$, of the PDF, $P_x(u|f_c)$, is obtained by conducting Fourier transform of Eq. (13) as,

$$\begin{aligned} F_x(\xi|f_c) &= \int_{-\infty}^{\infty} P_u(u|f_0)\exp\left(\frac{-\xi^2\sigma^2}{2}\right)\exp(-j\xi\gamma u)du \\ &= F_u(\gamma\xi|f_0)\exp\left(\frac{-\xi^2\sigma^2}{2}\right), \quad F_u(\xi|f) \equiv \mathcal{J}\left[P_u(u|f)\right] \end{aligned} \qquad \text{(A· 2)}$$

Symbol $\mathcal{J}$ [] denotes Fourier transform. By setting $f = f_0$ and $\gamma = 1$ in Eq. (A· 2),

$$F_x(\xi|f_0) = F_u(\xi|f_0)\exp\left(\frac{-\xi^2\sigma^2}{2}\right). \qquad \text{(A· 3)}$$

By replacing ξ with $\gamma\xi$ in Eq. (A· 3), and substituting $F_u(\gamma\xi|f_0)$ into Eq. (A· 2), we have the following:

$$F_x(\xi|f_c) = F_x(\gamma\xi|f_0)\exp\left(\frac{-\xi^2(1-\gamma^2)\sigma^2}{2}\right). \qquad \text{(A· 4)}$$

The inverse Fourier transform of Eq. (A· 4) yields convolution (14).

Appendix B

We use capital letters to indicate the amplitude on a dB scale, such as $X = 20\log_{10}(x)$. First, we should consider that there is a minimum amplitude $y_{\min} > 0$ (the lower bound of the dynamic range of the measuring receiver) that satisfies $APD(y) = 1$ for any $y < y_{\min}$. Hence, we divide integration in Eq. (15) into two parts:

$$\begin{aligned} &APD(y|f_c) = I_1 + I_2, \\ &I_1 \equiv \int_{-\infty}^{y\min} g(y-u|\sigma^2(1-\gamma^2))du, \\ &I_2 \equiv \int_{y\min}^{\infty} APD\left(\frac{u}{\gamma}|f_0\right)g(y-u|\sigma^2(1-\gamma^2))du. \end{aligned} \qquad \text{(A· 5)}$$

The first integral, I_1, is represented by the complimentary error function, and can be numerically calculated on a linear scale.

$$I_1 = \int_{-\infty}^{y\min} g(y-u|\sigma^2(1-\gamma^2))du = \frac{1}{2}erfc\left(\frac{y-y_{\min}}{\sqrt{2\pi\sigma^2(1-\gamma^2)}}\right). \tag{A·6}$$

The second integral, I_2, can be rewritten with Y, U, and Γ on a dB scale as follows:

$$I_2 = \int_{Y\min}^{\infty} APD\left(10^{\frac{-(U-\Gamma)}{20}} \,\middle|\, f_0\right)\cdot G(Y,U,\Gamma)\cdot\frac{1}{K}10^{\frac{-U}{20}}dU, \tag{A·7}$$

$$G(Y,U,\Gamma) \equiv \frac{1}{\sqrt{2\pi\sigma^2(1-10^{\frac{-\Gamma}{10}})}}\exp\left(\frac{-1}{2\sigma^2(1-10^{\frac{-\Gamma}{10}})}\cdot\left(10^{\frac{-Y}{20}}-10^{\frac{-U}{20}}\right)^2\right),$$

$$Y \equiv 20\log_{10}(y),\ U \equiv 20\log_{10}(u),\ \Gamma \equiv 20\log_{10}(\gamma),$$
$$K \equiv 20/\log_e(10).$$

When the amplitude is quantized by the step of ΔUon the dB scale, integration (A· 7) can be approximated by the following summation:

$$I_2 \cong \sum_{n=n_{\min}}^{n_{\max}} APD\left(10^{\frac{-(n\Delta U-\Gamma)}{20}} \,\middle|\, f_0\right)\cdot G(Y,n\Delta U,\Gamma)\cdot 10^{\frac{-n\Delta U}{20}}\frac{\Delta U}{K},$$
$$n_{\min}\Delta U = Y_{\min} = 20\log_{10}(y_{\min}),$$
$$n_{\max}\Delta U = Y_{\max} = 20\log_{10}(y_{\max}). \tag{A·8}$$

In summation (A· 8), the lower and upper bounds of the dynamic range of the APD measurement are denoted by $Y_{\min}$ and $Y_{\max}$ in dB, respectively. When γ is close to 1, the Gaussian PDF, $g(y-u,\sigma^2(1-\gamma^2))$, has a large peak and short width that may become narrower than the integration step size, $10^{-(n\Delta U/20)}\Delta U/K$, in the calculation of (A· 8). Since the integration of the PDF, g, never exceeds 1, the value of the term, $G(Y,n\Delta U,\Gamma)10^{-(n\Delta U/20)}\Delta U/K$, should be replaced by 1 if it becomes larger than 1.

Yasushi Matsumoto received the B.E., M.E. and Ph.D. degrees in electrical and communication engineering from Tohoku University, Sendai, Japan, in 1983, 1985, and 1998, respectively. In 1985, he started working at the Radio Research Laboratory (currently, National Institute of Information and Communications Technology). From 1990 to 1994, he was with National Space Development Agency of Japan (currently, Japan Aerospace Exploration Agency). From 1999 to 2005, he was an Associate Professor at Tohoku University. He is currently a research manager in the EMC group, NICT. His research interests include electromagnetic compatibility and wireless communications.

Kaoru Gotoh received the B.E., M.E. and Ph.D. degrees from the University of Electro-Communications, Tokyo, Japan, in 1996, 1998, and 2002, respectively. In 2003, she started working at the Communications Research Laboratory (currently, National Institute of Information and Communications Technology), where she has been engaged in research on EMC for radio communication systems.

Takashi Shinozuka received the B.S. degree in physics from Tokyo Metropolitan University, Tokyo, Japan, in 1971. He has been with the Radio Research Laboratory (currently, National Institute of Information and Communications Technology: NICT), since 1965, where he began researching millimeter wave propagation and remote sensing. From 1984 to 1985, he was with CRPE/CNET, Paris, France, working on studies in the same field. From 1996 to 1999, he was with the Electromagnetic Compatibility Laboratories, Sendai, Japan. From 1999 to 2007, he was a research manager at the Applied Electromagnetic Research Center, NICT. In 2007, he moved to Telecom Engineering Center (TELEC). His research interests are in the area of EMC measurement methods. He is an expert member of CISPR Subcommittee A.